



Fabrication of Negative Curvature Hollow Core Fiber

12

Muhammad Rosdi Abu Hassan

Contents

From Conventional Fibers to Photonics Crystal Fibers.....	530
Photonic Crystal Fiber.....	530
Background of Photonics Crystal Fiber.....	531
Development of Hollow Core Fiber.....	531
Development of Negative Curvature Hollow Core Fibers.....	533
The Importance Negative Curvature.....	534
Guiding Mechanism.....	535
Antiresonant Reflecting Optical Waveguide (ARROW).....	535
Marcatili and Schmelzter's Model.....	537
Coupled-Mode Model.....	538
Fabrication of Fiber.....	538
Fabrication of Negative Curvature Hollow Core Fiber.....	539
Stack and Draw.....	539
Design and Properties of Fiber.....	542
Conclusion.....	545
References.....	545

Abstract

In this chapter, we describe a review covering the development of the negative curvature hollow core fiber for the mid-IR region. The topics cover various types of hollow core fiber and their improvement made in term of attenuation of fiber, followed by a description of the guiding mechanism of the negative curvature hollow core fiber (NC-HCF) using antiresonant reflecting optical waveguide (ARROW) mechanism. Then, we present the general fabrication steps and the

M. R. Abu Hassan (✉)

Centre for Optical Fibre Technology (COFT), School of Electrical, Electronic Engineering,
Nanyang Technological University, Singapore, Singapore, Singapore
e-mail: muhdrodi22@gmail.com

fabrication process for negative curvature fiber. In the second part of the chapter, the design and properties of the hollow core applied in the other research work are presented.

Keywords

Fiber optics · Microstructured optical fiber · Hollow core fiber · Photonics crystal fiber

From Conventional Fibers to Photonic Crystal Fibers

Optical fiber is a key component of modern telecommunication technologies. This technology has been attracting much attention since the first single-mode fiber with loss <20 dB/km were made in 1970 (Kaiser and Astle 1974). Currently, conventional optical fiber forms the backbone of our global telecommunication network. Optical fibers perform very well in telecom applications but also are becoming more prominent for non-telecom technologies such as a laser, sensing, biomedical applications, and a host of other fields.

Even though conventional optical fibers have achieved a number of successes in the existing telecommunication technologies, there is a fundamental limitation which is related to the two materials structure used in the conventional fibers. There is a need to make a new class of fiber that can be as competitive as conventional fiber and offer significantly improved performance in some respects.

Photonic Crystal Fiber

Over the past 25 years, conventional optical fibers have revolutionized communications, transmitting more information over greater distances than could ever be achieved in copper wires, and are also vital in many technologies such as imaging endoscopes and high power laser transport for cutting and drilling applications.

Optical fibers have evolved into many types of structure to overcome the limitation of existing fiber. In 1996, Knight et al. fabricate new class of fiber using a single material which operates by total internal reflection as a guiding mechanism (Knight et al. 1996a). These new classes of fibers have the potential to outperform conventional fiber in certain aspects due to high flexibility to modify the structure and parameters. Some parameters of the fiber such as dispersion can be modified and tailored to suit the desire applications by designing different fiber structure.

An innovation was made by J.C. Knight and his group in 1996 where they managed to produce the photonic crystal fibers (PCF) which consist of a pure silica core surrounded by a silica-air photonic crystal material with a hexagonal symmetry (Knight et al. 1996b). Since then PCFs have captured research interests very rapidly due to the increasing demand for high-performance optical fibers. Two major limitations of conventional optical fibers that have led to the fabrication of photonic crystal fibers are the smallness of refractive-index difference, Δn which

causes bend loss (0.5 dB at 1550 nm in Corning SMF-28 for one turn around a mandrel 32 mm in diameter), and also the reliance on total internal reflection so that guidance in a hollow-core is impossible.

These new fibers, known collectively as microstructured fibers, can be made entirely from one type of glass as they do not rely on dopants for guidance. Instead, the cladding region is peppered with many small air holes that run the entire fiber length. These fibers are typically separated into two classes defined by the way in which they guide light:

1. Photonic band-gap fibers, in which guidance in a hollow core can be achieved via photonic band-gap effects.
2. Holey fibers, in which the core is solid and light is guided by a modified form of total internal reflection as the air holes lower the effective refractive index of the cladding relative to that of the solid core.

Background of Photonics Crystal Fiber

Fiber optics changed radically with the first demonstration (Knight et al. 1996a, 1997) of a new class of optical fibers that can have a variety of structures. Photonic Crystal Fibers (PCFs) as known as Microstructured Optical Fibers (MOFs), which have modified cladding structure in order to provide a high index contrast between core and cladding.

In 1974, it was first observed by P. Kaiser and H.W. Astle that low-loss single material fibers can be fabricated entirely from silica and the lowest steady-state loss of about 3 dB/km at a wavelength of 1.1 μm was obtained (Kaiser and Astle 1974). The basic idea explains that light could be trapped inside a hollow fiber core by creating a periodic wavelength-scale lattice of microscopic holes in the cladding glass – a “photonic crystal.” In 1996, Knight et al. reported the first photonic crystal fibers which consist of a pure silica core surrounded by a silica-air photonic crystal material with a hexagonal symmetry (Knight et al. 1997).

Then, followed the Endlessly Single Mode (ESM) PCF, which the fiber will guide only the fundamental mode (Birks et al. 1997). Since then PCFs have captured research interests very rapidly due to the increasing demand on high-performance optical fibers. By now, we have seen optical fibers that can have an endless variety of structures of PCF – large mode area (Knight et al. 1998a), dispersion controlled (Mogilevtsev et al. 1998), hollow core (Cregan 1999) birefringent (Ortigosa-Blanch et al. 2000), and multicore (Il 2000) (Fig. 1).

Development of Hollow Core Fiber

The hollow core optical waveguides refer to long cylindrical tubes and rectangular stripes made of dielectric or even metal. The potential of hollow core fiber made of a metal material for long-haul electromagnetic wave transmission theoretically has

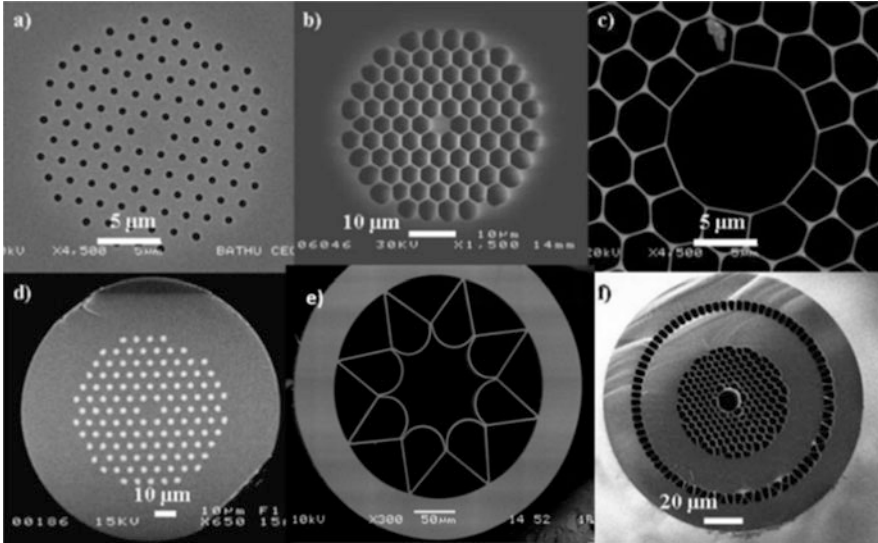


Fig. 1 Scanning electron microscope images of photonic crystal fibers: (a) solid core fiber, (b) high air-filling fraction solid core fiber, (c) hollow core fiber, (d) solid band-gap fiber consisting of a mixture of doped silica glasses, (e) a negative curvature fiber, and (f) double-clad hollow core fiber. This figure is reproduced from Russell (2003)

been proposed by Carson et al. (1936). Later, the feasibility of using the dielectric HCF in telecommunications has been studied by Marcatili and Schmeltzer (1964). They demonstrated analytically that the trade-off between modal leaky loss and a bending loss would fundamentally limit the application of dielectric hollow core fiber for long-haul optical signal transmission.

In the late twentieth century, the development of hollow-core photonic bandgap fiber (HC-PBG) speeded up the development of HCFs in both theory and applications immensely (Knight et al. 1998b; Russell 2006).

The state-of-the-art HC-PBGs was demonstrating extremely low transmission loss, comparable to that of commercial optical fibers (Roberts et al. 2005). They also have a very high damage threshold (Jaworski et al. 2013), very low group-velocity dispersion, and an optical nonlinearity that is many orders of magnitude less than that of competing fibers (Ouzounov et al. 2003).

Kagome fiber also is a part of HCF family. “Kagome” fiber was firstly reported in 2002 (Benabid et al. 2002). The Kagome fiber usually exhibits multiple transmission bands and overall covers a broader spectral range than HC-PBGs. Numerical simulations show that the “Kagome” lattice supports no photonic bandgap which makes the Kagome fiber distinct (Russell 2006; Benabid and Roberts 2011).

Another type of HC fiber is the negative curvature hollow core fiber (NC-HCF). With the simple single ring cladding design and negative curvature core wall, NC-HCF combine the strength and durability of silica with record low attenuation in the 3–4 μm spectral band, where their attenuation can be 10,000 times less

than that of bulk silica (Yu et al. 2012; Wheeler et al. 2014; Yu and Knight 2013; Bei et al. 2013; Kim et al. 2016). In this chapter, we describe a high performance of the negative curvature hollow core fiber (NC-HCF). Then, follow it by the characterization of the performance of NC-HCF.

Development of Negative Curvature Hollow Core Fibers

Negative curvature hollow-core fiber (NC-HCF) is a novel type of hollow core fiber, which is characterized by the negative curvature of core wall shape (Yu and Knight 2016). Such fiber exhibits multiple spectral transmission bands and can guide light in the hollow core with low attenuation over lengths of hundreds of meters. The exceptional qualities of NC-HCF, such as low transmission loss, extended transmission wavelength, and low latency and nonlinearity lend these fibers to a wide range of applications. The low-loss transmission windows in NC-HCF can span from visible to mid-infrared wavelengths (Yu and Knight 2016) and have been successfully applied in the transmission of high power lasers (Shephard et al. 2015), the design of mode-locked fiber lasers (Harvey et al. 2015), and study of nonlinear optics in gas (Wang et al. 2014a). Moreover, the simple structure of fiber cladding design allowing tuning flexibility of NC-HCF's design and dimension to meet specific wavelength and application requirement (Setti et al. 2013; Kolyadin et al. 2013; Belardi and Knight 2014b; Shiryayev 2015) (Fig. 2).

In 2010, Kagome hollow-core fiber with negative curvature core boundary results in lower attenuation than conventional kagome fiber (Wang et al. 2010). Results from that, a series of subsequent experiments have been done and confirmed the importance of core wall shape in the reduction of attenuation in such fibers (Wang et al. 2011). In 2011, a group led by Pryamikov attempt to fabricate the simple structure of hollow core which used only eight capillaries as a cladding. This fiber is the first NC-HCF made and operated in 3 μm wavelength (Pryamikov et al. 2011).

In 2013, Fei Yu reported transmission in 3.1-microns region with minimum attenuation of 34 dB/km. He called "core ice-cream shape of cladding" that has curvature towards the core that affects the attenuation of the fiber. Later, the fiber was successfully applied to invasive surgical laser procedure in delivering high energy microsecond pulses at 2.4 μm (Jaworski et al. 2013). Kolyadin et al. purposed simple design of the cladding structure of the NC-HCF to improve the attenuation in the mid-IR region. He reported the open boundary of core wall in NC-HCF, which is the contactless capillary in the cladding. He demonstrated low loss transmission of light in the mid-infrared spectrum range from 2.5 to 7.9 μm (Kolyadin et al. 2013). In 2014, Belardi et al. demonstrated significantly reduced the bending loss of the negative curvature fibers in 2014 (Belardi and Knight 2014a).

NC-HCF can be designed to guide light in an empty or gas-filled hollow core. Since as much as 99% of the optical power in these fibers can travel in air and not in the glass, they do not suffer from the same limitations to loss as conventional fibers and can exhibit drastically reduced optical nonlinearity, making them promising candidates for future ultra-low loss transmission fibers.

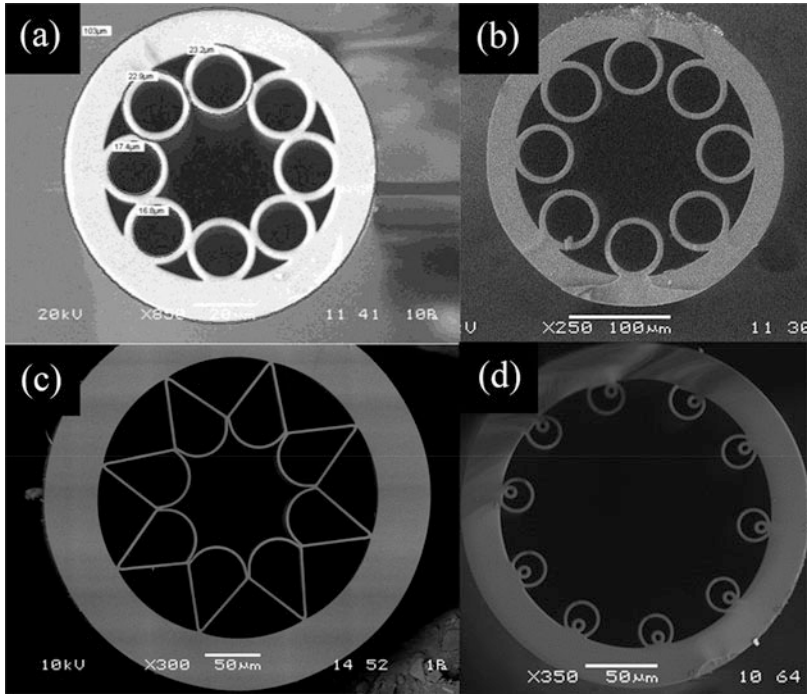


Fig. 2 SEM pictures of typical NC-HCFs: (a) NC-HCF made of silica, with capillaries in touch in the cladding [1]; (b) NC-HCF made of silica, with nontouching capillaries in the cladding [5]; (c) NC-HCF made of silica with ice cream cone-shape capillary in the cladding [3]; (d) NC-HCF made of silica, with non-touching capillaries. Extra capillaries are added to reduce the coupling between the core and cladding modes [33]

The NC-HCF has applied in many applications. Setti et al. were realized terahertz guidance in polymethyl-methacrylate in 2013 (Setti et al. 2013). Besides that, NC-HCF also has implemented in high power laser (Urich et al. 2013a, b) delivery and have been applied in the study of gas-light interaction.

We will present the steps to fabricate NC-HCF. We start with describing the guiding mechanism of the NC-HCF using Antiresonant Reflecting Optical Waveguide (ARROW) mechanism. Then, we will explain the fiber draw technique and the NC-HCF technique fabrication process. The characteristics of the NC-HCF will be described later.

The Importance Negative Curvature

NC-HCFs are characterized by the negative curvature of the core wall, which has been numerically and experimentally demonstrated to effectively reduce the attenuation. Numerical studies showed that in NC-HCF, an increase of negative

curvature influences the mode attenuation and even bending loss in a complex way (Belardi and Knight 2013). It has been confirmed that a large curvature of the core wall (small radius of curvature) can help decrease the overlap of core mode field with fiber materials to 10^{-4} . This has been experimentally and numerically demonstrated in silica NC-HCFs (Yu and Knight 2013; Belardi and Knight 2013). Despite recent efforts in the analytical analysis (Pryamikov 2014), the function of the core wall shape is not yet clear. It appears that both the properties of the high-index and of the low-index cladding modes are affected by the curvature.

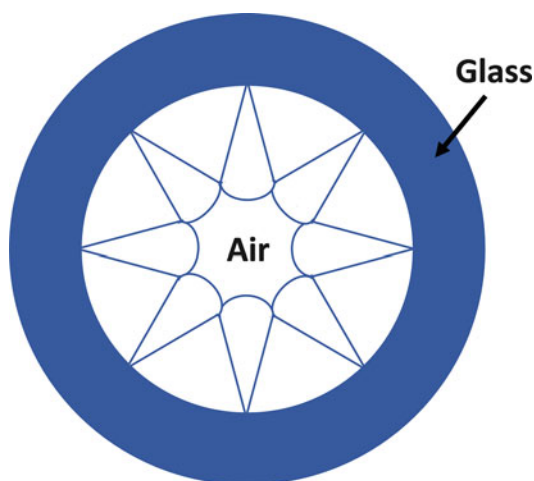
Guiding Mechanism

NC-HCF has a simple structure as shown in Fig. 3. It has no periodic cladding and does not possess a photonic bandgap, which explains the leaky nature of such fiber. The leaky nature and antiresonant guiding mechanism make it natural to compare NC-HCF with Kagome fiber. Both have multiple transmission bands and similar attenuation figures at comparable wavelengths (Debord et al. 2013; Alharbi et al. 2013).

Antiresonant Reflecting Optical Waveguide (ARROW)

The guiding mechanism of NC-HCF can be simply explained using Antiresonant Reflecting Optical Waveguide (ARROW) model. The ARROW model was firstly proposed in 1986 to explain the enhanced confinement in a planar waveguide with a series of high-low index regions forming the cladding (Duguay et al. 1986; White et al. 2002; Litchinitser et al. 2003). In 2002, it was used to provide a simple way to understand the light transmission in hollow-core photonic bandgap HC-PBG fiber

Fig. 3 Schematic representation of the cladding of a negative curvature hollow core fiber. The core is surrounded by the negative curvature cladding that guides the light in the core



regarding waveguide theory more rather than the tight binding theory (Litchinitser et al. 2002). Soon it was being applied to a range of microstructured HCF's.

The ARROW model is based on consideration of the individual modes of the high index regions. It approximates the cladding of HC-PBG as an array of high and low refractive index layers. Each higher refractive index layer can be considered as a Fabry–Perot resonator as shown in Fig. 4.

For one-dimensional case, when the wavelength of light in the core matches a resonant wavelength of the Fabry–Perot, the light will leak out of the core and confine in the high-index region, n_1 , but if they are in anti-resonance wavelength with high-index region, n_1 , the light will be confined back to the low-index core, n_2 , of the waveguide as shown in Fig. 4.

In the resonance in the 2-D waveguide, when the wavelength of light in the core matches a resonant wavelength of the Fabry–Perot cavity, the light will leak out of the core through the high index layer, n_1 . As the wavelength is far away from the resonance of the cladding, the light will be reflected back and more strongly confined in the core, n_2 of the waveguide. NC-HCF possesses multiple transmission bands, and the band edges are determined by the resonance wavelengths of cladding as described by the ARROW model (Fig. 5).

Fig. 4 Schematic diagrams of a one-dimensional anti-resonant planar waveguide (the core is running vertically). In these cases, high index regions, n_1 , are darker grey and the low index background material, n_2 , is white

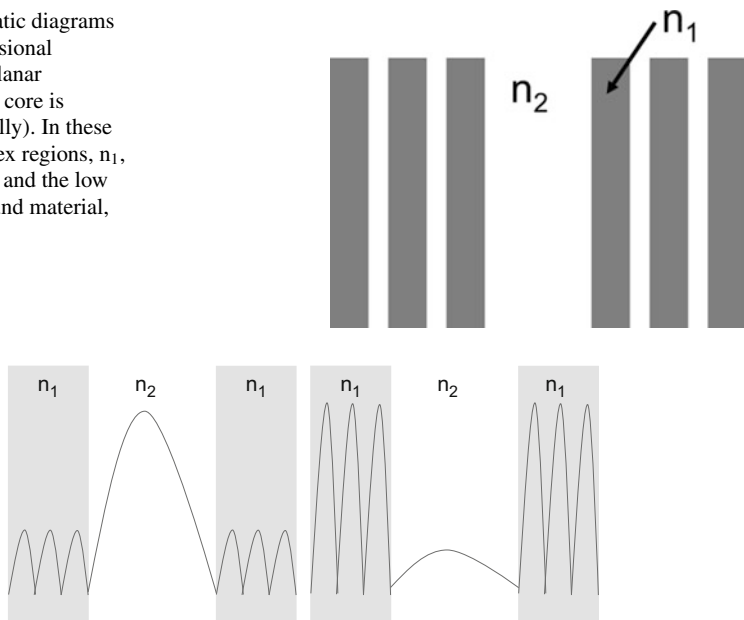


Fig. 5 Schematic representations of the intensity profile in the core region and first high index regions in the one-dimensional planar waveguide. In both cases, high index regions, n_1 , are darker grey and the low index background material n_2 is white; (a) is the anti-resonant case where light is confined to the core region by anti-resonant reflections and (b) is when the wavelength is close to a resonance of the high index regions corresponding to the peak transmission of the Fabry–Perot cavity

The ARROW model described the waveguide characteristics based on ray optics principle. ARROW cannot predict the loss magnitude or any other band details either. There are other models that can be used to explain the guidance mechanism of NC-HCFs and other leaky HCF, which is Marcatili and Schmeltzer model (Marcatili and Schmeltzer 1964), and the coupled mode model (Snyder and Love 2012). Although the ARROW model is far from perfection, it is still widely acknowledged as one of the most effective and frequently used models to understand leaky HCFs.

Marcatili and Schmeltzer's Model

In 1964, Marcatili and Schmeltzer first analytically studied the mode properties of the dielectric HCF (Marcatili and Schmeltzer 1964). In their pioneering work, they derived formulas of mode attenuation and bending loss, which revealed the basic properties of modes in HCFs. An HCF consists of a circular core surround by an infinite homogenous non-absorptive dielectric medium of the higher refractive index than the core material (usually gas/vacuum). Due to the inverted refractive index difference, total internal reflection cannot occur when the incident light from the core at the interface between the core and cladding. The partial reflectivity at the core boundary indicates an inevitable loss of light propagating in the core. The mode attenuation and the corresponding propagation constant are written as (Marcatili and Schmeltzer 1964);

$$A_{vm} = \left(\frac{u_{vm}}{2\pi} \right)^2 \frac{\lambda^2}{r^3} \text{Re}(V_v) \quad (1)$$

$$\beta_{vm} = \frac{2\pi}{\lambda} \left\{ n_{\text{core}} - \frac{1}{2} \left(\frac{u_{vm}}{2\pi} \right)^2 \left[1 + \text{Im} \left(\frac{(V_v \lambda)}{\pi r} \right) \right] \right\} \quad (2)$$

Here u_{vm} is the m th zero of the Bessel function J_{v-1} , and v and m are azimuthal and radial number of modes; λ is the wavelength; r is the core radius; n_{core} is the refractive index of core medium; and V_v is the constant determined by the cladding refractive index and mode order (Marcatili and Schmeltzer 1964). Equations (1) and (2) are the most basic formulas to understand modes in all leaky HCFs. As r/λ grows bigger, the attenuation of modes is quickly reduced. For a mode of a specific order, a higher propagation constant is required to satisfy the transverse resonance condition in a bigger core. Such larger core would give an increased glancing angle of light incident at the core boundary, which results in a higher Fresnel reflection. As a result, the mode in a larger core has a smaller attenuation. Marcatili and Schmeltzer's model fails when complex structures are introduced to the cladding of HCF. The multiple reflections from the structured cladding can reduce or increase the attenuation of leaky modes by constructive/destructive interference, and it also affects the dispersion of modes.

Coupled-Mode Model

The coupled-mode model applies coupled mode theory (Snyder and Love 2012) to analyze the properties of HCFs based on Marcatili and Schmeltzer's model. In real HCFs, the cladding is no longer an infinite and homogeneous medium but has a complex configuration of refractive index distribution. The cladding modes are a set of modes including both dielectric modes localized in the higher index regions and leaky air modes inside lower index regions (Couny et al. 2007; Vincetti and Setti 2010). In the coupled-mode model, the properties of core mode are interpreted as results of the longitudinal coupling with those cladding modes. This method was successfully applied in analyzing the formation of bandgaps in HC-PBG (Birks et al. 2006). By this method, inhibited coupling was proposed to explain the guidance in Kagome fiber (Benabid and Roberts 2011). In 2007, Argyros applied the coupled mode theory to the square lattice polymer HCF and quantitatively analyzed the formation of band edges of leaky HCF (Argyros and Pla 2007). They pointed out that the absolute phase matching is not necessary to achieve an effective coupling between the cladding and core modes. $\Delta\beta \sim 10^{-4}$ m was found to be the threshold to estimate the transmission band edge, which matched well with the experimental measurement (Argyros and Pla 2007). In 2012, Vincetti and Setti applied this method to NC-HCF and presented details of cladding mode features in NC-HCF (Vincetti and Setti 2010). Later, they used this method to demonstrate that the geometry of cladding elements was important to determine the confinement loss of HCFs. The polygonal shaped tube in the cladding adds extra loss due to the Fano-like coupling between the core and cladding modes (Vincetti and Setti 2012). This can be used to explain the different spectral features between NC-HCFs and Kagome fibers.

Fabrication of Fiber

Vapor-phase fabrication techniques are commonly used to fabricate conventional single mode fibers. In these processes, glass is created from high purity component gases using modified chemical vapor deposition (MCVD) process. The fabrication procedure for Photonic Crystal Fiber (PCF) differs radically from that used for conventional step index fiber as the microstructure usually comprises glass and air.

Photonic Crystal Fiber is unlike conventional fiber in that it is usually manufactured from only one material, the most commonly pure silica. As the guiding mechanism differs between the conventional optical fibers and photonic crystal fibers, the fabrication process also differs as the cladding requires a proper structural alignment in order to obtain PCFs with different advantages. Here, we are using the stack-and-draw method to fabricate novel PCF structures. We will discuss much detail about this and other techniques in the next section.

Fabrication of Negative Curvature Hollow Core Fiber

Negative Curvature Hollow Core Fiber (NC-HCF) is unlike conventional fiber is typically fabricated from only one material, the most commonly pure silica. The fabrication procedure for negative curvature hollow core fiber differs completely from that used for conventional step index fiber as the microstructure usually comprises glass and air. The simple one layer cladding of NC-HCF makes it easy to stack but require more attention to details when we draw to fiber. As the guiding mechanism differs between the conventional optical fibers, the fabrication process also differs as the cladding requires a proper structural arrangement to obtain high-performance NC-HCFs.

We are mainly using the stack-and-draw technique to fabricate our NC-HCF structures. This method is inherited from photonics crystal fiber (PCF) fabrication technique (Birks et al. 1995). There are other techniques to form the preform such as extrusion (Kiang et al. 2002; Kumar et al. 2002) and sol-gel casting (Bise and Trevor 2005; van Eijkelenborg et al. 2001) that are not discussed in this chapter.

Stack and Draw

The fibers are fabricated using an adapted stack and draw procedure starting from commercially available synthetic fused silica tubing. The main reason to use the stack and draw technique because, it offers high flexibility in designing the fiber structure, low cost, speed and repeatability. Moreover, this flexibility allows us to design a negative curvature fiber. Figure 6 shows a scanning electron microscope (SEM) images of a few types of NC-HCFs with different cladding structures.

The stack and draw technique and fiber drawing of NC-HCF that used in this work are shown in Fig. 7. In the stack and draw technique, the general step is to stack silica capillary tubes or solid silica rods into the desired pattern to produce a preform. The precision and uniformity while stacking capillaries and rods are essential because these will affect the properties and quality of fiber structure after the preform is drawn to fiber.

All materials used in fabrications presented in this thesis was F300, synthesized fused silica material from Heraeus which has a low concentration of OH group (Humbach et al. 1996). We started with two tubes different outer and inner diameter was used. Tube 1 has an outer diameter (OD) 16.03 mm and 12.27 mm of inner diameter. Tube 2 has an outer diameter (OD) 25.1 mm and 23.39 mm of inner diameter. Tube 1 will be a jacket tube, and tube two will draw to a smaller diameter to stack inside the Tube 2.

Stack

The fiber was fabricated using the stack and draw technique, by placing eight identical capillaries drawn from thin wall silica tube (Suprasil F300, Heraeus) inside a larger jacketing tube. To fabricate NC-HCF, two short capillaries (blue) or rods

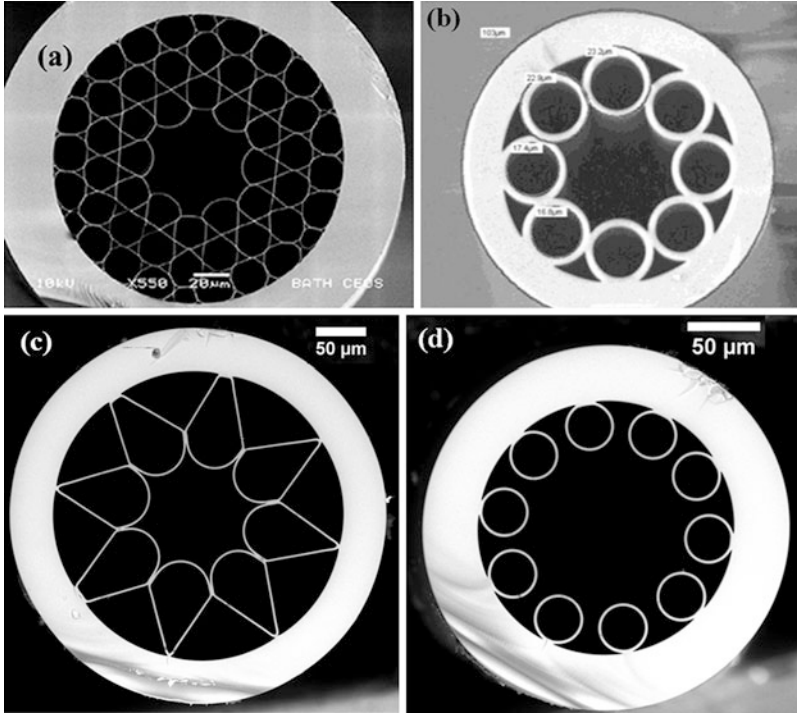


Fig. 6 Scanning electron microscope pictures of few types of negative curvature fiber: (a) hypocycloid-core Kagome hollow-core photonic crystal fiber (Wang et al. 2010), (b) is negative curvature fiber from Pryamikov group (Pryamikov et al. 2011), (c) ice cream shape NC-HCF from Yu et al. (2012), and (d) NC-HCF made of silica, with nontouching capillaries fabricated by Belardi and Knight (2014b)

need to be inserted in the core region at the ends of the stack to support the cladding and prevent the stack from collapsing and to make sure the stack tight and does not slip out during the drawing process as shown in the Fig. 7a.

Drawing of Cane

The cane is an intermediate preform which is drawn from the stack (Fig. 8b). The cane is essentially a complete optical waveguide but on the millimeter scale. The drawing of the cane is a necessary and important step in the fabrication of NC-HCF and other HCFs. One of the reason is to avoid a drastic scale change from the stack of the preform (centimeter scale) to final end-product (fiber) in micrometer scale. In the reference, Chen and Birks (2013) mention that preventing the structure from deformation becomes more problematic in the large-scale change. Conclusions, drawing fiber from the smaller cane more rather than a larger (in diameter) stack is a best practice to obtain a high-quality NC-HCFs. In our fabrication of NC-HCF, the cane size was usually about 3–4 cm in diameter.

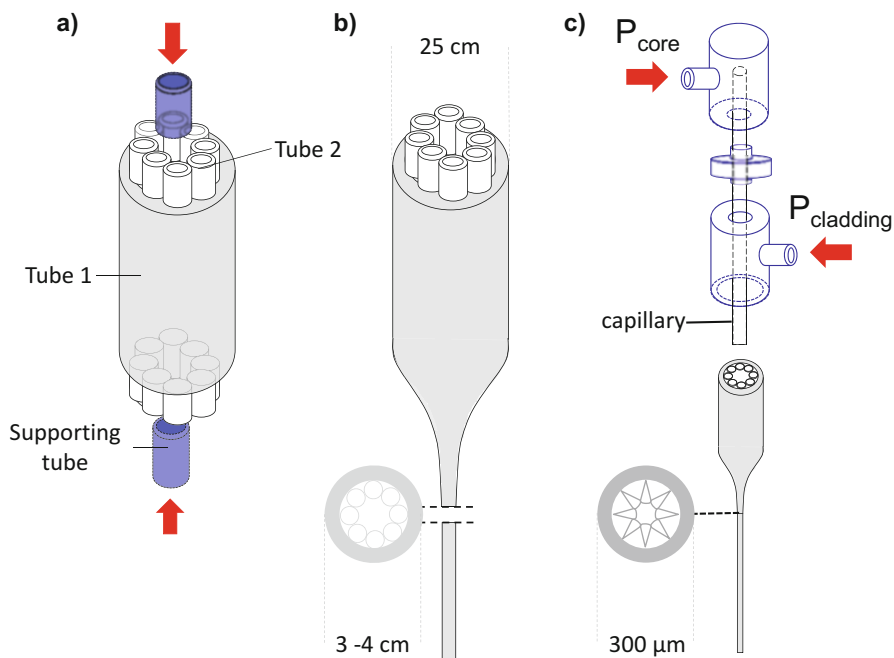


Fig. 7 Three stages of the stack and draw technique of NC-HCF. **(a)** The first stage is a stack to the desire cane. To maintain the cladding structure, two short capillaries (blue tube) are to insert on both ends as support. **(b)** Drawing of canes. The middle part of the stack without supporting capillaries is drawn into canes of smaller diameter (typically cane diameter is 3–4 cm). **(c)** Fiber fabrication from canes. Different pressures are applied to different regions of core and cladding

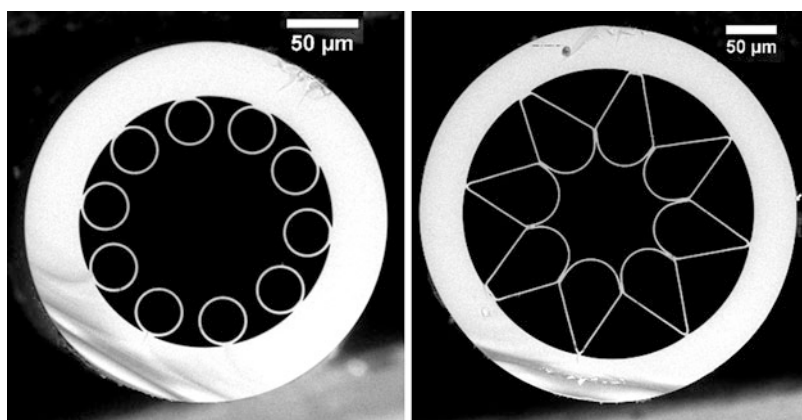


Fig. 8 Scanning electron micrographs of the two different forms of hollow fiber used in the laser system (Abu Hassan et al. 2016). Left: gain fiber with transmission at 1.53 and 3.1 μm wavelengths. Right: feedback fiber with low loss at 3.1 μm

Table 1 Fiber drawing parameters to obtain NC-HCF for 3.16 μm wavelength

Feed rate (mm/min)	Draw speed (m/min)	Temperature ($^{\circ}\text{C}$)	P core (kPa)	P cladding (kPa)
50	6.6	1910	0.1	6

Drawing of Fiber

Next, the cane is drawn to the fiber size using the fiber drawing tower as shown in Fig. 7c. In this process, the end of the cane is fitted to the brass metal holder. This custom made holder has a small hole to apply pressure into the cane to maintain air holes from collapse in the drawing process. The pure nitrogen used for pressurization. The pressurization is crucial not only to avoid the air holes from collapse during the drawing process but also the key to the formation of the negative curvature core wall. The negative curvature core wall can affect the attenuation and the mode profile of the hollow core fiber.

While the fiber has been drawn, the feed speed of the cane, the draw speed of the fiber, the furnace temperature, and the gas pressure must be carefully adjusted, or the fine structure of fiber can be easily deformed otherwise. In the drawing stage, polymer material will be coated around the final fiber for protection and enhancement of the mechanical strength of the optical fiber. The fabrication parameter to obtain the NC-HCF are shown in this book are presented in Table 1.

Design and Properties of Fiber

Fiber Design

The silica-based hollow fibers used in the experiments in the Abu Hassan et al. (2016) offer a complementary approach to fiber lasers in the mid-IR and are shown in Fig. 8. The work in Abu Hassan et al. (2016), we used two different hollow core fibers with slightly different designs. First, is the hollow core with un-touching capillaries in the cladding and second is the “ice cream shape” in the cladding. This fiber will be our gain fiber and feedback fiber respectively. The similarity features of both fibers are negative curvature core boundary wall. The negative curvature core boundary provides a lower attenuation in interested wavelength for both fibers (Yu and Knight 2013).

First, the anti-resonant hollow core fiber used as a gain fiber was fabricated and reported in Belardi and Knight (2014a). This fiber is chosen because it has low attenuation at the pump band around 1.53 μm and low attenuation at the lasing wavelength around 3.1 μm as shown in Fig. 7. The gain fiber has a core diameter of $\sim 109 \mu\text{m}$; an outer diameter of $\sim 233 \mu\text{m}$, an average “cladding capillaries” diameter of 27.9 μm , and a silica wall thickness of $\sim 2.4 \mu\text{m}$ (Fig. 9).

Secondly, the negative curvature fiber (NCF) was specially designed to provide the lowest possible attenuation at the lasing wavelength. The NCF was used as a feedback fiber. It has a core diameter of $\sim 95 \mu\text{m}$, an outer diameter of $\sim 357 \mu\text{m}$, as shown in Fig. 10b. We will discuss more technique used to obtain NCF attenuation in the next section.

Fig. 9 The measured transmission loss of the anti-resonant HC-PCF at shorter (solid line, top x-axis) and longer (blue dash line, bottom x-axis) wavelength. This figure is from Wang et al. (2014b)

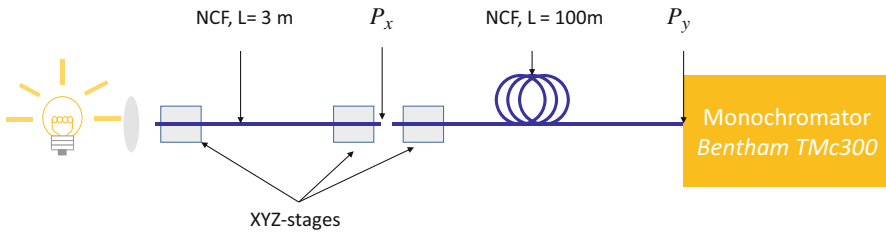
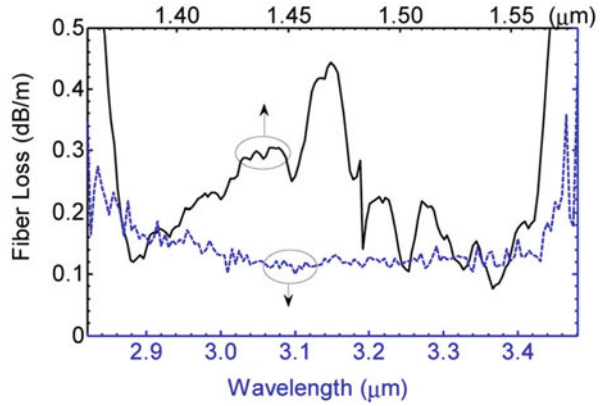


Fig. 10 Schematic of the modified version of the conventional cut-back technique to determine attenuation for feedback fiber

Attenuation Measurement: Cutback Method

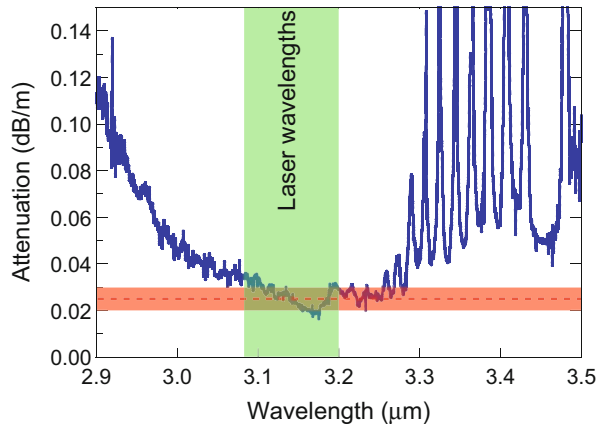
Attenuation is among of the main characteristics of the fiber. Attenuation of an optical fiber is the loss of optical power as a result of leakage, scattering, bending, and other loss mechanisms as the light travel through the fiber. The cutback method is often used for measuring the total attenuation of an optical fiber. The cutback method involves comparing the optical power transmitted through a longer piece of fiber to the power transmitted through a shorter piece of the fiber.

The cutback method requires that a test fiber of known length (L) be cut back to a shorter length (L_c). The cutback method begins by measuring the output power, P_y , of the test fiber of known length (L). Without disturbing the input conditions, the test fiber is cut back to a shorter length (L_c). The output power, P_x , of the short test fiber (L_c) is then measured, and the fiber attenuation is calculated. The attenuation of the cut piece can be determined by:

$$\alpha \text{ (dB/m)} = \frac{10 \log_{10} (P_x/P_y)}{L - L_c} \tag{3}$$

The standard cutback technique is a destructive technique which means the fiber under test to determining certain optical fiber transmission characteristics, such as attenuation and bandwidth. To avoid cutting the feedback fiber, we have measured

Fig. 11 Attenuation curve for the feedback fiber showing attenuation of 0.025 ± 0.005 dB/m over the laser wavelength band. Sharp features at $3.3 \mu\text{m}$ and beyond arise from small quantities of HCl gas present in the fiber core. The pink band indicates the uncertainty in the measurement of minimum attenuation



the fiber attenuation accurately by using a modified version of the conventional cut-back technique in which we use low loss butt-coupling (see Fig. 11), which is repeatable, instead of cutting the fiber, which is not. Butt-coupling has a very low loss (<0.1 dB) in these fibers because of the low numerical aperture, large core size and absence of Fresnel reflections. The uncertainty in the loss measurement is ± 5 dB/km. The fiber was loosely coiled on the bench with a bend radius of 40 cm to avoid additional loss caused by bending.

In this section, all the cut-back measurements were performed by using a tungsten lamp; it has a broad spectrum from near-UV to mid-IR. In our experiments, all the spectra were measured and recorded by the optical spectrum analyzer (OSA) *Ando AQ 6315A* (wavelength range from 350 to 1750 nm) and a scanning monochromator *Bentham TMc300* (wavelength range from 250 nm to $5.4 \mu\text{m}$).

Figure 11 shows the attenuation curve for the feedback fiber, showing attenuation of 0.025 ± 0.005 dB/m over the laser wavelength band. Sharp features at $3.3 \mu\text{m}$ and beyond arise from small quantities of HCl gas present in the fiber core. The presence of trace amounts of HCl gas in our fiber would appear to be reasonable given that our starting material is F300 synthetic fused silica, which contains 1450 ppm of chlorine (Haken et al. 2000), and our measurement is over 100 m in length. We can remove those absorption lines by purging the fiber with nitrogen.

The red color band indicates the uncertainty in the measurement of attenuation. Then, we remeasure the attenuation using single wavelength laser to validate the accuracy of our measurement. Our feedback fiber (ice-cream cone shape) has one of the lowest attenuations reported for an optical fiber in this spectral band (Abu Hassan et al. 2016).

The disadvantage of the tungsten lamp is its limited luminance especially at wavelengths above $3 \mu\text{m}$ in the mid-infrared spectral region. To validate our attenuation measurement for feedback fiber using a tungsten lamp, we used our own CW $3 \mu\text{m}$ laser as a source to re-measure the fiber attenuation. The cut-back measurements were performed by replacing the tungsten lamp with our stable CW

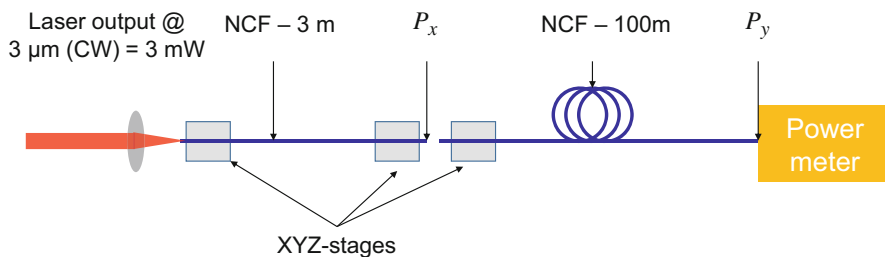


Fig. 12 Schematic of the modified version of the conventional cut-back technique used to determine attenuation for feedback fiber

Table 2 Readings of the attenuation of the NC-HCF using single wavelength laser

P_x (mW)	P_y (mW)	Loss (dB/m)
0.600	0.303	0.0297
0.605	0.309	0.0292
0.615	0.304	0.0306

3 μm laser and the output measured using a power meter as shown in Fig. 12. Measurements of optical powers were performed using a thermal power meter (*Ophir 3A-SH*).

Table 2 lists the readings of the attenuation at 3.12 μm using stable CW laser. We recorded three readings with the average attenuation 0.0298 dB/m, slightly higher compared to the attenuation using tungsten lamp due to a smaller fiber coil radius causing the bending loss increase. However, the attenuation is still in the acceptable range and shows an agreement with the previous measurement.

Conclusion

This chapter shows the study of design and properties of negative curvature fiber. The step by step fabrication method of NC-HCF using stack and draw was shown. The cut-back measurement is the main method to determine the attenuation of NC-HCF experimentally.

References

- M.R. Abu Hassan et al., Cavity-based mid-IR fiber gas laser pumped by a diode laser. *Optica* **3**(3), 218 (2016). <https://www.osapublishing.org/abstract.cfm?URI=optica-3-3-218>. Accessed 7 July 2016
- M. Alharbi et al., Hypocycloid-shaped hollow-core photonic crystal fiber. Part II: cladding effect on confinement and bend loss. *Opt. Express* **21**(23), 28609–28616 (2013). <http://www.osapublishing.org/viewmedia.cfm?uri=oe-21-23-28609&seq=0&html=true>. Accessed 26 Jan 2016

- A. Argyros, J. Pla, Hollow-core polymer fibres with a Kagome lattice: potential for transmission in the infrared. *Opt. Express* **15**(12), 7713 (2007). <https://www.osapublishing.org/oe/abstract.cfm?uri=oe-15-12-7713>. Accessed 7 Dec 2016
- J. Bei et al., Reduction of scattering loss in fluoroindate glass fibers. *Opt. Mater. Express* **3**(9), 1285 (2013). <http://www.opticsinfobase.org/abstract.cfm?URI=ome-3-9-1285>
- W. Belardi, J.C. Knight, Effect of core boundary curvature on the confinement losses of hollow antiresonant fibers. *Opt. Express* **21**(19), 21912 (2013). <https://www.osapublishing.org/oe/abstract.cfm?uri=oe-21-19-21912>. Accessed 7 Dec 2016
- W. Belardi, J.C. Knight, Hollow antiresonant fibers with low bending loss. *Opt. Express* **22**(8), 10091–10096 (2014a). <http://www.osapublishing.org/viewmedia.cfm?uri=oe-22-8-10091&seq=0&html=true>. Accessed 15 Oct 2015
- W. Belardi, J.C. Knight, Hollow antiresonant fibers with reduced attenuation. *Opt. Lett.* **39**(7), 1853–1856 (2014b). <http://www.osapublishing.org/viewmedia.cfm?uri=ol-39-7-1853&seq=0&html=true>. Accessed 26 Jan 2016
- F. Benabid, P.J. Roberts, Linear and nonlinear optical properties of hollow core photonic crystal fiber. *J. Mod. Opt.* **58**(2), 87–124 (2011). <http://www.tandfonline.com/doi/abs/10.1080/09500340.2010.543706>. Accessed 7 Dec 2016
- F. Benabid et al., Stimulated Raman scattering in hydrogen-filled hollow-core photonic crystal fiber. *Science* **298**(5592), 399–402 (2002)
- T.A. Birks, P.J. Roberts, P.S.J. Russell, D.M. Atkin, T.J. Shepherd, et al., Full 2-D photonic bandgaps in silica/air structures. *Electron. Lett.* **31**(22), 1941–1943 (1995)
- T.A. Birks, J.C. Knight, P.S. Russell, Endlessly single-mode photonic crystal fiber. *Opt. Lett.* **22**(13), 961–963 (1997). <http://www.ncbi.nlm.nih.gov/pubmed/18185719>
- T.A. Birks, G.J. Pearce, D.M. Bird, Approximate band structure calculation for photonic bandgap fibres. *Opt. Express* **14**(20), 9483–9490 (2006). <http://www.ncbi.nlm.nih.gov/pubmed/19529335>
- R.T. Bise, D.J. Trevor, Sol-gel derived microstructured fiber: fabrication and characterization, in *OFC/NFOEC Technical Digest. Optical Fiber Communication Conference, 2005*, vol. 3 (2005), p. 3. Available at: <http://ieeexplore.ieee.org/lpdocs/epic03/wrapper.htm?arnumber=1501298>
- J.R. Carson, S.P. Mead, S.A. Schelkunoff, Hyper-frequency wave guides – mathematical theory. *Bell Syst. Tech. J.* **15**(2), 310–333 (1936). <http://ieeexplore.ieee.org/lpdocs/epic03/wrapper.htm?arnumber=6772987>. Accessed 7 Dec 2016
- Y. Chen, T.A. Birks, Predicting hole sizes after fibre drawing without knowing the viscosity. *Opt. Mater. Express* **3**(3), 346 (2013). <http://www.osapublishing.org/viewmedia.cfm?uri=ome-3-3-346&seq=0&html=true>. Accessed 7 Mar 2016
- F. Couny et al., Identification of Bloch-modes in hollow-core photonic crystal fiber cladding. *Opt. Express* **15**(2), 325 (2007). <https://www.osapublishing.org/abstract.cfm?URI=oe-15-2-325>. Accessed 7 Dec 2016
- R.F. Cregan, Single-mode photonic band gap guidance of light in air. *Science* **285**(5433), 1537–1539 (1999). <http://www.sciencemag.org/cgi/doi/10.1126/science.285.5433.1537>. Accessed 7 Nov 2013
- B. Debord et al., Hypocycloid-shaped hollow-core photonic crystal fiber. Part I: arc curvature effect on confinement loss. *Opt. Express* **21**(23), 28597–28608 (2013). <http://www.osapublishing.org/viewmedia.cfm?uri=oe-21-23-28597&seq=0&html=true>. Accessed 26 Jan 2016
- M.A. Duguay et al., Antiresonant reflecting optical waveguides in SiO₂-Si multilayer structures. *Appl. Phys. Lett.* **49**(1), 13 (1986). <http://scitation.aip.org/content/aip/journal/apl/49/1/10.1063/1.97085>. Accessed 26 Jan 2016
- U. Haken et al., Refractive index of silica glass: influence of fictive temperature. *J. Non-Cryst. Solids* **265**(1–2), 9–18 (2000). <http://www.sciencedirect.com/science/article/pii/S0022309399006973>. Accessed 8 Mar 2016
- C. Harvey et al., in *Reducing Nonlinear Limitations of Ytterbium Mode-Locked Fibre Lasers with Hollow-Core Negative Curvature Fibre*. CLEO: 2015 (OSA, Washington, DC, 2015),

- p. STh1L.5. Available at: https://www.osapublishing.org/abstract.cfm?uri=CLEO_SI-2015-STh1L.5. Accessed 23 Mar 2016
- O. Humbach et al., Analysis of OH absorption bands in synthetic silica. *J. Non-Cryst. Solids* **203**, 19–26 (1996). <http://www.sciencedirect.com/science/article/pii/0022309396003298>. Accessed 7 Mar 2016
- D.O. II, Experimental study of dual-core photonic crystal fibre. *Electron. Lett.* **36**(16), 1358–1359 (2000)
- P. Jaworski et al., Picosecond and nanosecond pulse delivery through a hollow-core negative curvature fiber for micro-machining applications. *Opt. Express* **21**(19), 22742–22753 (2013). <http://www.ncbi.nlm.nih.gov/pubmed/24104161>
- P. Kaiser, H.W. Astle, Low-loss single-material fibers made from pure fused silica. *Bell Syst. Tech. J.* **53**(6), 1021–1039 (1974). <http://ieeexplore.ieee.org/lpdocs/epic03/wrapper.htm?arnumber=6774079>. Accessed 16 Jan 2019
- K.M. Kiang et al., Extruded singlemode non-silica glass holey optical fibres. *Electron. Lett.* **38**(12), 546 (2002). http://digital-library.theiet.org/content/journals/10.1049/el_20020421
- W.H. Kim et al., Recent progress in chalcogenide fiber technology at NRL. *J. Non-Cryst. Solids* **431**, 8–15 (2016). <https://doi.org/10.1016/j.jnoncrysol.2015.03.028>
- J.C. Knight et al., All-silica single-mode optical fiber with photonic crystal cladding. *Opt. Lett.* **21**(19), 1547 (1996a). <https://www.osapublishing.org/abstract.cfm?URI=ol-21-19-1547>. Accessed 15 Mar 2018
- J.C. Knight et al., Pure silica single-mode fiber with hexagonal photonic crystal cladding. *Proc. Opt. Fiber Commun. Conference* (1996b), pp. 339–342
- J.C. Knight et al., All-silica single-mode optical fiber with photonic crystal cladding: errata. *Opt. Lett.* **22**(7), 484–485 (1997). <http://www.ncbi.nlm.nih.gov/pubmed/18183242>
- J.C. Knight et al., Large mode area photonic crystal fibre. *Electron. Lett.* **34**(13), 1347 (1998a). <http://link.aip.org/link/ELLEAK/v34/i13/p1347/s1&Agg=doi>
- J.C. Knight et al., Photonic band gap guidance in optical fibers. *Science* **282**(5393), 1476–1478 (1998b)
- A.N. Kolyadin et al., Light transmission in negative curvature hollow core fiber in extremely high material loss region. *Opt. Express* **21**(8), 9514–9519 (2013). <http://www.osapublishing.org/viewmedia.cfm?uri=oe-21-8-9514&seq=0&html=true>. Accessed 21 Jan 2016
- V.V.R. Kumar et al., Extruded soft glass photonic crystal fiber for ultrabroad supercontinuum generation. *Opt. Express* **10**(25), 1520–1525 (2002). <http://www.ncbi.nlm.nih.gov/pubmed/19461687>
- N.M. Litchinitser et al., Antiresonant reflecting photonic crystal optical waveguides. *Opt. Lett.* **27**(18), 1592 (2002). <http://www.osapublishing.org/viewmedia.cfm?uri=ol-27-18-1592&seq=0&html=true>. Accessed 26 Jan 2016
- N.M. Litchinitser et al., Resonances in microstructured optical waveguides. *Opt. Express* **11**(10), 1243–1251 (2003). <http://www.ncbi.nlm.nih.gov/pubmed/19465990>
- E.A.J. Marcatili, R.A. Schmelzter, Hollow metallic and dielectric waveguides for long distance optical transmission and lasers. *Bell Syst. Tech. J.* **43**(4), 1783–1809 (1964). <http://ieeexplore.ieee.org/lpdocs/epic03/wrapper.htm?arnumber=6773550>. Accessed 28 Dec 2015
- D. Mogilevtsev, T.a. Birks, P.S. Russell, Group-velocity dispersion in photonic crystal fibers. *Opt. Lett.* **23**(21), 1662–1664 (1998). <http://www.ncbi.nlm.nih.gov/pubmed/18091876>
- A. Ortigosa-Blanch et al., Highly birefringent photonic crystal fibers. *Opt. Lett.* **25**(18), 1325–1327 (2000). <http://www.ncbi.nlm.nih.gov/pubmed/18066205>
- D.G. Ouzounov et al., Generation of megawatt optical solitons in hollow-core photonic band-gap fibers. *Science* **301**(5640), 1702–1704 (2003). <http://www.ncbi.nlm.nih.gov/pubmed/14500976>. Accessed 5 Mar 2013
- A.D. Pryamikov, in *Negative Curvature Hollow Core Fibers: Design, Fabrication, and Applications*, ed. by S. Ramachandran (2014), p. 89610I. Available at: <http://proceedings.spiedigitallibrary.org/proceeding.aspx?doi=10.1117/12.2041653>. Accessed 7 Dec 2016
- A.D. Pryamikov et al., Demonstration of a waveguide regime for a silica hollow – core microstructured optical fiber with a negative curvature of the core boundary in the spectral region

- >3.5 μm . *Opt. Express* **19**(2), 1441–1448 (2011). <http://www.ncbi.nlm.nih.gov/pubmed/21263685>
- P.J. Roberts et al., Ultimate low loss of hollow-core photonic crystal fibres. *Opt. Express* **13**(1), 236 (2005). <https://www.osapublishing.org/oe/abstract.cfm?uri=oe-13-1-236>. Accessed 7 Dec 2016
- P. Russell, Photonic crystal fibers. *Science* **299**(5605), 358–362 (2003). <http://www.ncbi.nlm.nih.gov/pubmed/12532007>. Accessed 16 Jan 2019
- P.S.J. Russell, Photonic-crystal fibers. *J. Lightwave Technol.* **24**(12), 4729–4749 (2006). <http://ieeexplore.ieee.org/document/4063429/>. Accessed 7 Dec 2016
- V. Setti, L. Vincetti, A. Argyros, Flexible tube lattice fibers for terahertz applications. *Opt. Express* **21**(3), 3388–3399 (2013). <http://www.ncbi.nlm.nih.gov/pubmed/23481799>; <http://www.osapublishing.org/viewmedia.cfm?uri=oe-21-3-3388&seq=0&html=true>. Accessed 26 Jan 2016
- J.D. Shephard et al., Silica hollow core microstructured fibers for beam delivery in industrial and medical applications. *Front. Phys.* **3**, 24 (2015). <http://journal.frontiersin.org/article/10.3389/fphy.2015.00024/abstract>. Accessed 23 Mar 2016
- V.S. Shiryayev, Chalcogenide glass hollow-core microstructured optical fibers. *Front. Mater.* **2**, 24 (2015). <http://journal.frontiersin.org/article/10.3389/fmats.2015.00024/abstract>. Accessed 13 Nov 2015
- A.W. Snyder, J. Love, *Optical Waveguide Theory* (Springer, New York, 2012). <https://books.google.com/books?hl=en&lr=&id=DCXVBwAAQBAJ&pgis=1>. Accessed 20 Apr 2016
- A. Ulrich et al., Flexible delivery of Er:YAG radiation at 2.94 μm with negative curvature silica glass fibers: a new solution for minimally invasive surgical procedures. *Biomed. Opt. Express* **4**(2), 193–205 (2013a). <http://www.osapublishing.org/viewmedia.cfm?uri=boe-4-2-193&seq=0&html=true>. Accessed 15 Apr 2016
- A. Ulrich et al., Silica hollow core microstructured fibres for mid-infrared surgical applications. *J. Non-Cryst. Solids* **377**, 236–239 (2013b). <http://www.sciencedirect.com/science/article/pii/S0022309313001166>. Accessed 20 Apr 2016
- M. van Eijkelenborg et al., Microstructured polymer optical fibre. *Opt. Express* **9**(7), 319–327 (2001). <http://www.ncbi.nlm.nih.gov/pubmed/19516722>
- L. Vincetti, V. Setti, Waveguiding mechanism in tube lattice fibers. *Opt. Express* **18**(22), 23133–23146 (2010). <http://www.ncbi.nlm.nih.gov/pubmed/21164654>. Accessed 7 Dec 2016
- L. Vincetti, V. Setti, Extra loss due to Fano resonances in inhibited coupling fibers based on a lattice of tubes. *Opt. Express* **20**(13), 14350 (2012). <https://www.osapublishing.org/oe/abstract.cfm?uri=oe-20-13-14350>. Accessed 7 Dec 2016
- Y.Y. Wang et al., in *Low loss broadband transmission in optimized core-shape Kagome hollow-core PCF*. Conference on Lasers and Electro-Optics (CLEO) and Quantum Electronics and Laser Science Conference (QELS), 2010 (2010), pp. 4–5
- Y.Y. Wang et al., Low loss broadband transmission in hypocycloid-core Kagome hollow-core photonic crystal fiber. *Opt. Lett.* **36**(5), 669–671 (2011)
- Z. Wang, F. Yu, et al., Efficient 1.9 μm emission in H₂-filled hollow core fiber by pure stimulated vibrational Raman scattering. *Laser Phys. Lett.* **11**(10), 105807 (2014a). <http://iopscience.iop.org/article/10.1088/1612-2011/11/10/105807>. Accessed 3 Feb 2016
- Z. Wang, W. Belardi, et al., Efficient diode-pumped mid-infrared emission from acetylene-filled hollow-core fiber. *Opt. Express* **22**(18), 21872 (2014b). <https://www.osapublishing.org/oe/abstract.cfm?uri=oe-22-18-21872>
- N.V. Wheeler et al., Low-loss and low-bend-sensitivity mid-infrared guidance in a hollow-core-photonic-bandgap fiber. *Opt. Lett.* **39**(2), 295–298 (2014). <http://www.ncbi.nlm.nih.gov/pubmed/24562130>
- T.P. White et al., Resonance and scattering in microstructured optical fibers. *Opt. Lett.* **27**(22), 1977–1979 (2002). <http://www.ncbi.nlm.nih.gov/pubmed/18033417>

- F. Yu, J.C. Knight, Spectral attenuation limits of silica hollow core negative curvature fiber. *Opt. Express* **21**(18), 21466–21471 (2013). <http://www.ncbi.nlm.nih.gov/pubmed/24104021>; <http://www.osapublishing.org/viewmedia.cfm?uri=oe-21-18-21466&seq=0&html=true>. Accessed 28 Sept 2015
- F. Yu, J. Knight, Negative curvature hollow core optical fiber. *IEEE J. Sel. Top. Quantum Electron.* **22**(2), 1–11 (2016). <http://opus.bath.ac.uk/47694/3/07225120.pdf>. Accessed 25 Jan 2016
- F. Yu, W.J. Wadsworth, J.C. Knight, Low loss silica hollow core fibers for 3–4 μm spectral region. *Opt. Express* **20**(10), 11153–11158 (2012). <http://www.ncbi.nlm.nih.gov/pubmed/22565738>